STRENGTH CURVES FOR WEB CRIPPLING DESIGN
First approach for stainless steel hat sections based on numerical analyses

Marina Bock, Esther Real, Enrique Mirambell

Universitat Politècnica de Catalunya (UPC), Department of Construction Engineering, Spain
marina.bock@upc.edu, esther.real@upc.edu, enrique.mirambell@upc.edu

INTRODUCTION

Hat sections belong to the family of cold-formed steel structural members and are often used as secondary structural members undergoing local transverse forces while supporting roof or wall cladding. The webs of such sections have high height-to-thickness ratio; hence web crippling usually controls their design. During last years, stainless steel structural applications have been growing due to their combination of material properties, durability and appeal. Despite significant progress has been made in the development of design rules for this material, the European stainless steel design code EN1993-1-4 [1] refers to the carbon steel cold-formed members provisions EN1993-1-3 [2] to predict web crippling resistance. Web crippling is a rather complex local instability governed by many geometric and material parameters as well as type of loading: interior one flange (IOF), exterior one flange (EOF), interior two flange (ITF) and exterior two flange (ETF). As a result, the design provisions to predict web crippling strength provide empirical equations based on test data adjustment that lack theoretical background. Although some theoretical models are available to predict web crippling strength on carbon steel hat sections [3, 4], they are too cumbersome for hand calculation purposes. Some background related to web crippling of stainless steel cross-sections can be found in [5] and [6]. On the other hand, the treatment of most of the failure modes within the European design provisions are based on the so called strength curves, providing different slenderness-based functions $\chi(\bar{\lambda})$ for a given instability. A recent investigation [7] has proof that such a slenderness based approach is possible for web crippling design of plate channel steel beams. The present study is intended to extend the method by proposing $\chi(\bar{\lambda})$ strength curves to predict web crippling strength of ferritic stainless steel hat sections undergoing IOF and EOF loading. The investigation has been based on numerical and experimental data tested in other institutions [8]. A comparison between this proposal and predicted resistances by EN1993-1-3 [2] and American standards [9] is also presented.

1 FINITE ELEMENT MODEL

1.1 Modeled tests and FE description

The finite element software Abaqus v6.11 was employed to model 8 tests on ferritic stainless steel hat sections subjected to web crippling (4 tests undergoing IOF and 4 tests undergoing EOF) carried out at VTT Technical Research Centre of Finland [8]. It is important to mention that the configuration of these tests was intended to reproduce the web crippling response at the vicinity of the intermediate support (IOF) and the end support (EOF) of a continuous beam in the most general case where the lips of the hat section are in the upper position. *Fig. 1* presents the dimensions of the hat sections where h is the web height, b is the flange width, t is the thickness, c is the lip length and r_i, r_m and R are the internal, centreline and external bending radius respectively. *Table 1* presents the reported material properties in [8] where E is the material Young modulus, $\sigma_{0.2}$ is the 0.2% proof stress, σ_u and ε_u are the ultimate stress and its corresponding ultimate strain and finally, n and m are the first and second strain-hardening parameters respectively. The centreline dimensions, the specimen's length, L, the support dimensions, S, the bearing plate length, s_s, as well as the clear distance between the steel plate under the force and the end support, e, (see *Fig. 2*) of these cross-sections [8] are presented in *Table 2* where important information is provided by the beam labeling. Considering ITH_10 as an example, I is the load configuration, TH stands for Top Hat and 10 is ten times the nominal thickness of the cross-section in mm. The geometry of these ferritic stainless

steel hat sections was discretized by using the four-node doubly curved shell element with reduced integration S4R. The mesh used in the model was studied to achieve accurate results whilst minimizing computational time. The whole stress-strain (engineering) data curve was obtained employing the compound two-stage Mirambell and Real model [10]. The true stress and plastic true strain were specified in the numerical model. The model was intended to simulate the experimental test configurations [8] as close as possible and therefore, different boundary conditions were ascribed for both loading conditions (IOF and EOF). More details are provided in the following sections.

Table 1. Material properties of the modeled specimens [8]

Nominal thickness (mm)	E (GPa)	$\sigma_{0.2}$ (MPa)	n	σ_u (MPa)	m	ε_u
1	200	359	23.1	479	1.46	0.0170
1.5	191	322	26.1	475	1.21	0.0160
2	193	372	23.0	489	1.30	0.0164
3	180	297	23.5	445	1.22	0.0160

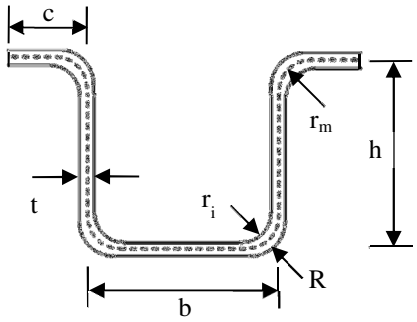

Fig. 1. Definition of symbols in the cross-section

Table 2. Centreline dimensions and length of the modeled specimens. Experimental [8] and numerical results

Beam	h (mm)	b (mm)	c (mm)	t (mm)	r_m (mm)	L (mm)	S (mm)	s_s (mm)	e (mm)	$F_{u,test}$ (kN)	$R_{u,test}$ (kN)	$F_{u,num}$ (kN)	$R_{u,num}$ (kN)	$F_{u,num}/F_{u,test}$
ITH_10	71.09	72.89	24.17	0.99	1.65	399	50	25	-	10.01	5.00	10.19	5.09	1.018
ITH_15	70.73	70.56	24.11	1.53	1.9	399	50	25	-	20.73	10.37	21.04	10.70	1.032
ITH_20	70.08	69.72	24.02	1.99	2.4	399	50	25	-	34.84	17.42	34.99	17.50	1.004
ITH_30	69.95	68.86	23.82	2.95	4.25	399	50	25	-	55.01	27.51	57.89	28.95	1.052
ETH_10	71.05	72.85	24.15	0.99	1.65	399	50	25	75	10.05	3.59	9.96	3.56	0.991
ETH_15	70.84	70.47	24.03	1.53	1.9	399	50	25	75	21.06	7.52	20.36	7.27	0.967
ETH_20	70.52	69.65	23.98	1.99	2.4	399	50	25	75	36.29	12.96	33.91	12.11	0.934
ETH_30	69.39	68.86	23.74	2.94	4.25	399	50	25	75	58.90	21.04	53.72	19.18	0.912
												Mean		0.989
												COV		0.046

1.2 Boundary conditions in the Internal One Flange (IOF) loading

The steel plate (s_s) that applies the transverse force was assumed to be a rigid plate controlled by a reference point (RP) in which all the degrees of freedom were restrained except the vertical displacement. The interface between the flange (slave surface, extended up to the corners) of the stainless steel section and this bearing plate (master surface) was modeled as a contact pair (surface-to-surface) assuming frictionless response in the tangential direction and hard response in the normal one. The transverse compressive load was applied by means of an imposed vertical displacement in the reference point (RP) of the bearing plate. Additional rigid plates (S) were placed on both edges in contact with the lips of the cross section to model support conditions. Those plates were also controlled by a reference point provided with appropriate boundary conditions to allow rotation due to bending. To avoid possible local instabilities and slide in those support regions, the ends of the flat parts of both the web and flange were restrained against vertical and horizontal displacement as well as rotation in the x-axis along the same support length to model the wooden blocks placed in such parts during testing (see *Fig. 2a*).

1.3 Boundary conditions in the External One Flange (EOF) loading

The steel plate (S) that applies the transverse force was modeled in the same way as in the IOF loading. This plate was fixed to the lips of the hat section by screw clamps in the experimental test [8] which were modeled by tying the surfaces in contact. The end bearing support (s_s) was modeled

as a rigid surface and a contact pair was used to model the interface with the specimen. In the experimental test [8], the distortional deformation of the further end support was restrained by placing a wooden block between the webs of the cross-section which was accounted for in the FE model by defining the hat section as a rigid body with its corresponding reference point in its center of mass. Appropriate boundary conditions were applied to the corresponding controlling reference points of the rigid surface and the rigid body which were free to rotate in the y-axis (see *Fig. 2b*).

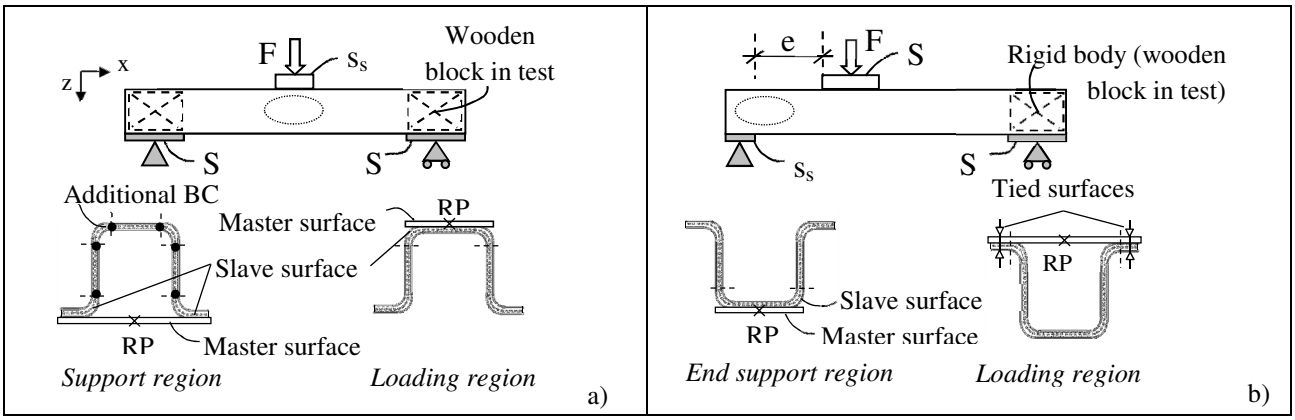

Fig. 2. FE model details for the a) IOF loading and b) EOF loading

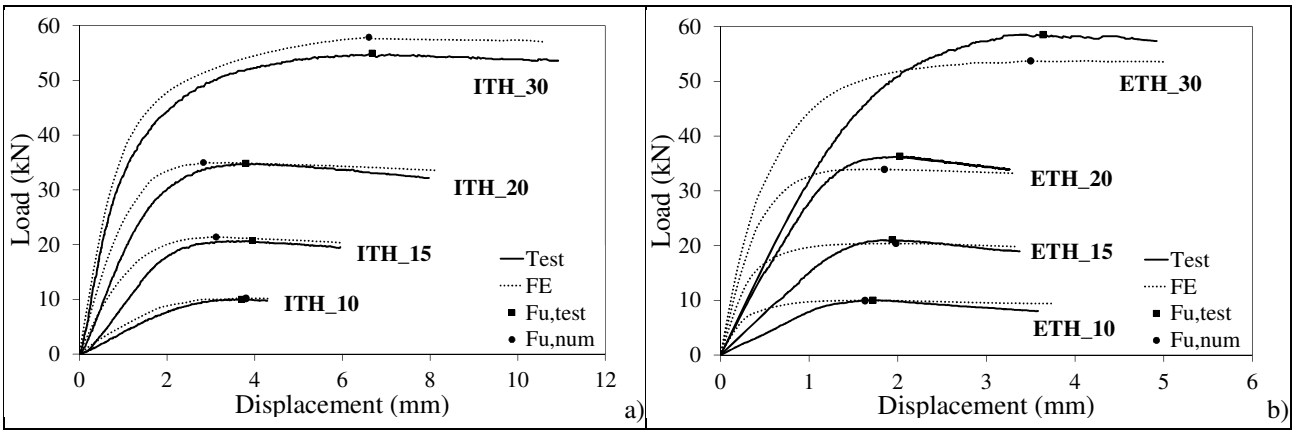

Fig. 3. Load-displacement response of the beams subjected to a) IOF and b) EOF loading

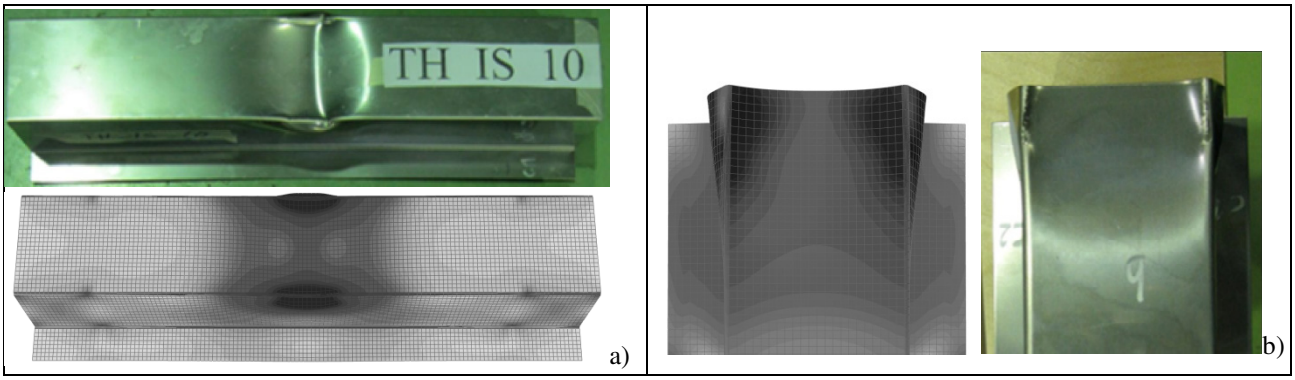

Fig. 4. Typical web crippling failure modes in a) IOF loading and b) EOF loading

1.4 FE model validation

Fig. 3 presents a comparison between the experimental and the numerical load-displacement response in which the corresponding ultimate loads have also been highlighted whereas *Table 2* presents the applied ultimate experimental load, $F_{u,test}$, the web crippling resistance per web, $R_{u,test}$, the ultimate numerical load, $F_{u,num}$, the ultimate numerical resistance per web, $R_{u,num}$, as well as the ratio numerical to experimental. In line with other studies [11, 12], it is also observed in these load-displacement responses a strong discrepancy in the stiffness due to the FE model sensitiveness to

boundary conditions. On the other hand, overall good agreement between test and numerical ultimate loads was achieved with an average value of the ratio FE to experimental of 0.989 and coefficient of variation (COV) of 0.046. This leads to conclude that this FE model is reliable and suitable to conduct further parametric studies. Some experimental and numerical failure modes are presented in *Fig. 4* for both IOF and EOF loading.

2 PARAMETRIC STUDIES

2.1 Purpose and numerical models

Having validated the numerical model, parametric studies were conducted with the aim to study the influence of the different parameters affecting web crippling capacity and determine the adequacy of a slenderness-based approach formulation for hat sections subjected to web crippling in both IOF and EOF loading conditions. The adopted material in this parametric study was ferritic stainless steel with the following material properties: E=200GPa, $\sigma_{0.2}$=350MPa, n=15, σ_u=450MPa, m=3 and ε_u=0.15. A total of 7 different sections undergoing both loading conditions were considered whose centreline dimensions in mm were (hxbxcxtxr_m): 30x30x17x1x1.5, 50x50x20x1.5x2, 70x70x25x1.5x2, 80x50x20x1.5x2, 100x50x20x1.5x2, 50x80x20x1.5x2 and 100x100x25x1.5x2. The specimen's length (L), the bearing plate (s_s) and the support plates (S) were 400, 25 and 50mm respectively. Additional beams were modeled to study the influence of: the bending radius (r_m= 1.5, 2.5 and 3mm); the length (L=600 and 800mm); the bearing length (s_s=12.5 and 50mm for IOF whereas 10 and 35mm for EOF); the thickness (t=0.5, 0.75, 1 and 2mm); and the clear distance (e) for the EOF loading condition, which originally was 25mm, was increased up to 75mm.

2.2 Types of analyses

The essence of the slenderness-based approaches provided in current design rules is that a member fails in a way involving buckling and yielding. On the basis of this principle, different strength curves are provided. These curves depend on the relative slenderness $\bar{\lambda}$ and the so called reduction factor χ given in *Eq.(1)*. Consequently, 3 types of analyses were performed in this study to determine the corresponding resistances per web: an elastic buckling analysis to obtain the elastic critical resistance R_{cr}; a first order plastic analysis (material non-linear) to determine the first order plastic resistance R_{pl}; and a fully material and geometrical non-linear analysis to determine the web crippling strength R_u. In total, about 190 numerical analyses were conducted.

$$\chi = \frac{R_u}{R_{pl}};\ \bar{\lambda} = \sqrt{\frac{R_{pl}}{R_{cr}}} \tag{1}$$

2.3 Results

Fig. 5 presents the variation of the reduction factor χ with the relative slenderness $\bar{\lambda}$ based on numerical results for both modeled and tested [8] beams. For both loading configurations, the results exhibit values of the reduction factor less than 1.0 which indicates that the first order plastic load, R_{pl}, is suitable to define this variable for web crippling design. Moreover, the reduction factor χ decreases for higher relative slenderness $\bar{\lambda}$ which evidences the contribution of elastic critical buckling resistance, R_{cr}, in the web crippling strength and confirms that the given expression in *Eq. (1)* for the relative slenderness $\bar{\lambda}$ is appropriate, in line with [7]. Hence these observations lead to conclude that such a slenderness based approach based on $\chi(\bar{\lambda})$ strength curves is also possible for web crippling design of ferritic stainless steel hat sections subjected to IOF and EOF loading.

3 PROPOSED STRENGTH CURVES AND COMPARISON WITH OTHER FORMULATIONS

A first approach is presented in this section by providing two strength curves given in *Eq. (2)* and *Eq. (3)* for IOF and EOF loading respectively where $\bar{\lambda}$ is determined according to *Eq. (1)*. These curves are plotted in *Fig. 5* in which strength curves for plain steel channels [7] were also depicted

for comparison purposes. Although this first proposal requires employment of numerical analyses to determine both first order plastic resistance R_{pl} and critical buckling resistance R_{cr}, it is strongly believed that further theoretical predictive models could achieve good agreement with numerical data.

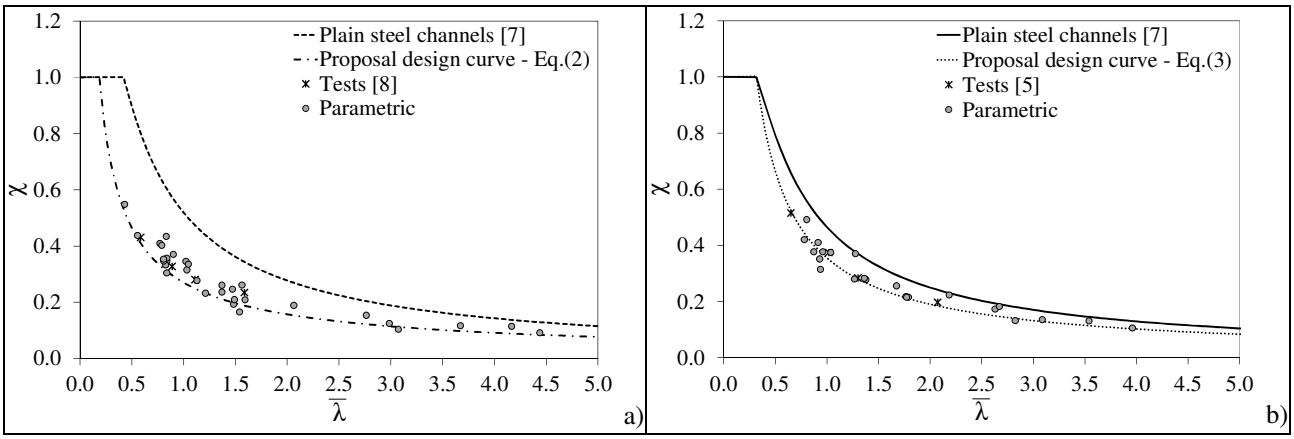

Fig. 5. Numerical results and proposed strength curves for a) IOF and b) EOF loading

$$R_{u,pro} = R_{pl}\left(\frac{0.270}{\overline{\lambda}^{0.78}}\right) \text{ for IOF loading} \tag{2}$$

$$R_{u,pro} = R_{pl}\left(\frac{0.355}{\overline{\lambda}^{0.90}}\right) \text{ for EOF loading} \tag{3}$$

Table 3. Experimental to predicted resistance ratios by different methods for the tested specimens [8]

Beam	R_{cr} (kN)	R_{pl} (kN)	$R_{u,EC}$ (kN)	$R_{u,ASCE}$ (kN)	$R_{u,pro}$ (kN)	$R_{u,test}/R_{u,EC}$	$R_{u,test}/R_{u,ASCE}$	$R_{u,test}/R_{u,pro}$	Beam	R_{cr} (kN)	R_{pl} (kN)	$R_{u,EC}$ (kN)	$R_{u,ASCE}$ (kN)	$R_{u,pro}$ (kN)	$R_{u,test}/R_{u,EC}$	$R_{u,test}/R_{u,ASCE}$	$R_{u,test}/R_{u,pro}$
ITH_10	8.62	21.73	3.20	3.32	4.09	1.56	1.50	1.22	ETH_10	4.17	17.91	1.39	1.53	3.29	2.58	2.35	1.09
ITH_15	30.94	38.12	6.19	6.80	9.49	1.67	1.53	1.09	ETH_15	15.21	25.71	2.85	3.49	7.21	2.64	2.151	1.04
ITH_20	67.70	53.41	10.29	11.65	15.82	1.69	1.50	1.10	ETH_20	33.05	34.29	4.97	6.23	11.97	2.61	2.079	1.08
ITH_30	195.97	67.20	15.27	17.65	27.54	1.80	1.56	0.99	ETH_30	95.76	40.48	8.56	12.26	21.72	2.46	1.716	0.99
					Mean	1.68	1.52	1.10						Mean	2.57	2.07	1.05
					COV	0.05	0.02	0.07						COV	0.03	0.11	0.03

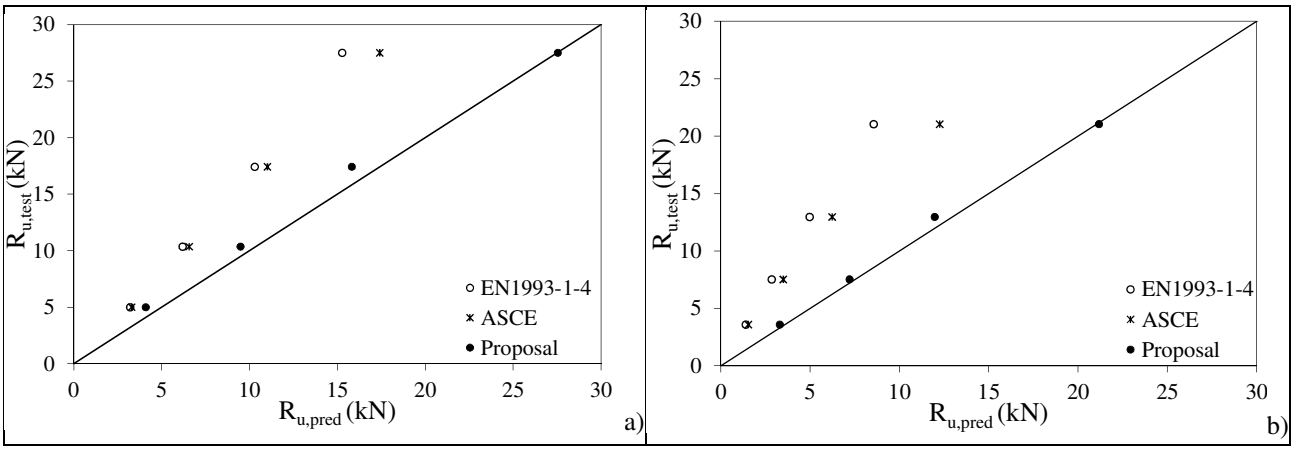

Fig. 6. Predicted resistances by different formulations for a) IOF and b) EOF loading

Table 3 presents the obtained numerical values of R_{pl} and R_{cr} for the tested beams [8] as well as the ratio experimental resistance $R_{u,test}$ to predicted strength by EN1993-1-3 [2] $R_{u,EC}$, ASCE [7] $R_{u,ASCE}$ and proposal by *Eqs. (2-3)* $R_{u,pro}$. The results show overly conservative strengths provided by design provisions whereas more accurate results and small scatter are achieved by this proposal for both

loading conditions. A graphical comparison of this improvement is given in *Fig. 6* for this experimental data. The whole results from the parametric study cannot all be given in this short article, though the mean values and COV for the ratio numerical, $R_{u,num}$, to predictive formulations are presented in *Table 4*.

Table 4. Numerical to predicted resistance ratio by different methods for the parametric study

	IOF			EOF		
	$R_{u,num}/R_{u,EC}$	$R_{u,num}/R_{u,ASCE}$	$R_{u,num}/R_{u,prop}$	$R_{u,num}/R_{u,EC}$	$R_{u,num}/R_{u,ASCE}$	$R_{u,num}/R_{u,prop}$
Mean	1.83	1.81	1.15	2.23	2.18	1.06
COV	0.22	0.26	0.11	0.18	0.20	0.11

4 ACKNOWLEDGMENTS

The research leading to these results has received funding from the European Community's Research Fund for Coal and Steel (RFCS) under Grant Agreement No. RFSR-CT-2010-00026, Structural Applications for Ferritic Stainless Steels and from Ministerio de Ciencia e Innovación to the Project BIA 2012-36373. The first author is grateful to the Secretaria d'Universitats i de Recerca del Departament d'Economia i Coneixement de la Generalitat de Catalunya i del Fons Social Europeu for their financial contribution. The authors gratefully acknowledge all the experimental information provided by Asko Talja and Petr Hradil from VTT. They would also like to thank Professor Feng Zhou from Tongji University for the provided support in the FE model.

REFERENCES

[1] EN1993-1-4, 2006. "Eurocode 3: Design of steel structures - Part 1.4: General rules - Supplementary rules for stainless steel", CEN.

[2] EN1993-1-3, 2006. "Eurocode 3: Design of steel structures - Part 1.3: General rules - Supplementary rules for cold-formed members and sheeting", CEN.

[3] Bakker MCM., Stark JWB., 1994. "Theoretical and Experimental Research on Web Crippling of Cold-Formed Flexural Steel Members", *Thin Walled Structures*, Vol. 18, No. 4, pp. 261-290.

[4] Hofmeyer H., Kerstens JGM., Snijder HH., Bakker MCM., 2001. "New prediction model for failure of steel sheeting subject to concentrated load (web crippling) and bending", *Thin Walled Structures*, Vol. 39, No. 9, pp. 773–796.

[5] Zhou F., Young B., 2008. "Web Crippling of Cold-Formed Stainless Steel Tubular Sections", *Advances in Structural Engineering*, Vol. 11, No. 6, pp 679-691.

[6] Bock M., Arrayago I., Real E., Mirambell E., 2013. "Study of web crippling in ferritic stainless steel cold formed sections", *Thin Walled Structures*, Vol. 69, No. 4, pp 29-44.

[7] Duarte APC., Silvestre N., 2013. "A New Slenderness-based Approach for the Web Crippling Design of Plain Channel Steel Beams", *International Journal of Steel Structures*, Vol. 3, No. 3, pp. 421-434.

[8] Talja A., Hradil P., 2011. "SAFSS Work package 2: Model calibration tests - Test Report", VTT Technical Research Centre of Finland.

[9] American Society of Civil Engineers (ASCE), 2002. "Specification for the design of cold-formed stainless steel structural members (SEI/ASCE 8-02)".

[10] Mirambell E., Real E., 2000. "On the calculation of deflections in structural stainless steel beams: an experimental and numerical investigation", *Journal of Construction Steel Research*, Vol. 54, No. 1, pp. 109–33.

[11] Hofmeyer H., 2000. "Combined web crippling and bending moment failure of first-generation trapezoidal steel sheeting", PhD-thesis, Eindhoven University of Technology, Faculty of Architecture, Department of Structural Design, The Netherlands, ISBN 90-6814-114-7.

[12] Kaitila, O, 2004. "Web crippling of cold-formed thin-walled steel cassettes", Doctoral dissertation, Helsinki University of Technology Laboratory of Steel Structures publications TKK-TER-30, Finland.

STRENGTH CURVES FOR WEB CRIPPLING DESIGN
First approach for stainless steel hat sections based on numerical analyses

Marina Bock, Esther Real, Enrique Mirambell

Universitat Politècnica de Catalunya (UPC), Department of Construction Engineering, Spain
marina.bock@upc.edu, esther.real@upc.edu, enrique.mirambell@upc.edu

KEYWORDS: stainless steel, hat sections, web crippling, reduction function, concentrated load

ABSTRACT

Web crippling is a local instability that causes cold-formed sections to become unstable when a concentrated load is applied transversally to the cross-section. The European design rules for stainless steels EN1993-1-4 [1] refers to the standards for carbon steel cold-formed sections EN1993-1-3 [2] to determine the web crippling ultimate capacity in which different expressions are presented according to the cross-sectional number of webs. For the fundamental case of hat sections (cross-sections with two or more webs), a single expression is codified which is in essence an empirical equation based on curve fitting given different coefficients. During the last years, research has been focused on improving this expression but overlooking the philosophy of a $\chi(\bar{\lambda})$ strength curve in which are based most of the instability verifications of the European design provisions. Some background related to web crippling of stainless steel cross-sections can be found in [3] and [4]. The purpose of this paper is to assess if this slenderness-based approach is suitable to determine the ultimate resistance of stainless steel hat sections subjected to web crippling. The appraisal will be based on numerical simulations performed in Abaqus and experimental results found in the literature [5]. A comparison of the results with current design rules according to European [2] and American standards [6] is also presented. Two new expressions to predict web crippling strength of ferritic stainless steel hat sections are proposed in the present study.

CONCLUSIONS

Experimental tests on ferritic stainless steel hat sections subjected to web crippling under IOF and EOF loading conditions [5] have been modeled with Abaqus v6.11 and complemented with parametric studies to assess whether a new approach based on the so called $\chi(\lambda)$ strength curves given in *Eq. (1)* is appropriate for web crippling design. These numerical results have shown that such approach is possible and therefore, two different strength curves given in *Eq. (2)* and *Eq. (3)* for IOF and EOF loading respectively have been proposed. Such proposed strength curves are presented in *Fig. 1* where the corresponding numerical reduction factor χ and relative slenderness $\bar{\lambda}$ are depicted for the tested specimens and the parametric analysis. In addition, strength curves proposed in other studies [7] have also been plotted in this figure for comparison purposes.

$$\chi = \frac{R_u}{R_{pl}};\ \bar{\lambda} = \sqrt{\frac{R_{pl}}{R_{cr}}} \tag{1}$$

where R_{cr} is the elastic buckling resistance per web,
R_{pl} is the first order plastic resistance per web,
R_u is the web crippling strength per web.

$$R_{u,pro} = R_{pl}\left(\frac{0.270}{\bar{\lambda}^{0.78}}\right) \text{ for IOF loading} \tag{2}$$

$$R_{u,pro} = R_{pl}\left(\frac{0.355}{\bar{\lambda}^{0.90}}\right) \text{ for EOF loading} \tag{3}$$

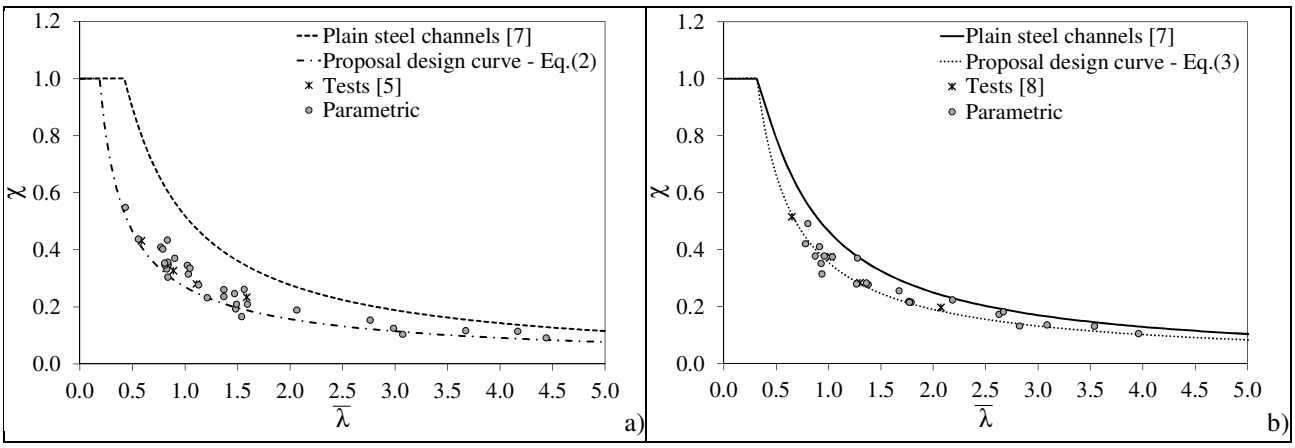

Fig. 1. Results and proposed strength curves based on numerical values of P_{pl}, P_{cr} and P_u for a) IOF and b) EOF

None theoretical predictive model is proposed in this study to determine either R_{cr} or R_{pl}; hence this first approach requires FE simulations to determine these aforementioned resistances. The former must be determined by means of an eigenvalue analysis whereas the latter requires a first order plastic analysis. Overall the predicted resistances for both loading configurations, $R_{u,pro}$, provide more precise results with low scatter compared to [2] $R_{u,EC}$, and [6] $R_{u,ASCE}$, as shown in *Table 1*.

Table 1. Numerical to predicted resistance ratio by different methods for the parametric study and tests [5]

	IOF			EOF			IOF			EOF		
	$R_{u,test}/R_{u,EC}$	$R_{u,test}/R_{u,ASCE}$	$R_{u,test}/R_{u,prop}$	$R_{u,test}/R_{u,EC}$	$R_{u,test}/R_{u,ASCE}$	$R_{u,test}/R_{u,prop}$	$R_{u,num}/R_{u,EC}$	$R_{u,num}/R_{u,ASCE}$	$R_{u,num}/R_{u,prop}$	$R_{u,num}/R_{u,EC}$	$R_{u,num}/R_{u,ASCE}$	$R_{u,num}/R_{u,prop}$
Mean	1.68	1.52	1.10	2.57	2.07	1.05	1.83	1.81	1.15	2.23	2.18	1.06
COV	0.05	0.02	0.07	0.03	0.11	0.03	0.22	0.26	0.11	0.18	0.20	0.11

ACKNOWLEDGMENTS

The research leading to these results has received funding from the European Community's Research Fund for Coal and Steel (RFCS) under Grant Agreement No. RFSR-CT-2010-00026, Structural Applications for Ferritic Stainless Steels and from Ministerio de Ciencia e Innovación to the Project BIA 2012-36373. The first author is grateful to the Secretaria d'Universitats i de Recerca del Departament d'Economia i Coneixement de la Generalitat de Catalunya i del Fons Social Europeu for their financial contribution. The authors gratefully acknowledge all the experimental information provided by Asko Talja and Petr Hradil from VTT. They would also like to thank Professor Feng Zhou from Tongji University for the provided support in the FE model.

REFERENCES

[1] EN1993-1-4, 2006. "Eurocode 3: Design of steel structures - Part 1.4: General rules - Supplementary rules for stainless steel", CEN.

[2] EN1993-1-3, 2006. "Eurocode 3: Design of steel structures - Part 1.3: General rules - Supplementary rules for cold-formed members and sheeting", CEN.

[3] Zhou F., Young B., 2008. "Web Crippling of Cold-Formed Stainless Steel Tubular Sections", *Advances in Structural Engineering*, Vol. 11, No. 6, pp 679-691.

[4] Bock M., Arrayago I., Real E., Mirambell E., 2013. "Study of web crippling in ferritic stainless steel cold formed sections", *Thin Walled Structures*, Vol. 69, No. 4, pp 29-44.

[5] Talja A., Hradil P., 2011. "SAFSS Work package 2: Model calibration tests - Test Report", VTT Technical Research Centre of Finland.

[6] American Society of Civil Engineers (ASCE), 2002. "Specification for the design of cold-formed stainless steel structural members (SEI/ASCE 8-02)".

[7] Duarte APC., Silvestre N., 2013. "A New Slenderness-based Approach for the Web Crippling Design of Plain Channel Steel Beams", *International Journal of Steel Structures*, Vol. 3, No. 3, pp. 421-434.